Scientific Reports

https://doi.org/10.1038/s41598-026-39854-0

Article in Press

Role of the ABCG2 transporter in the biodistribution of the food-borne uremic toxin *p*-cresyl sulfate

Received: 16 December 2025

Accepted: 9 February 2026

Published online: 21 February 2026

Cite this article as: Millán-García A., Álvarez-Fernández L., Velasco-Díez M. *et al.* Role of the ABCG2 transporter in the biodistribution of the food-borne uremic toxin *p*-cresyl sulfate. *Sci Rep* (2026). https://doi.org/10.1038/s41598-026-39854-0

Alicia Millán-García, Laura Álvarez-Fernández, Miriam Velasco-Díez, Diana Huertas-Álvarez, Álvaro López-García, Álvaro Fuente, Gracia Merino & Esther Blanco-Paniagua

Role of the ABCG2 transporter in the biodistribution of the food-borne uremic toxin *p*-cresyl sulfate

Alicia Millán-García[a], Laura Álvarez-Fernández[a], Miriam Velasco-Díez[a], Diana Huertas-Álvarez[a], Álvaro López-García[a], Álvaro de la Fuente[a], Gracia Merino[a] and Esther Blanco-Paniagua[a]*.

[a]Department of Biomedical Sciences–Physiology, Faculty of Veterinary Medicine, Animal Health Institute (INDEGSAL), 24071, Universidad de León, Campus de Vegazana, León, Spain.

***Corresponding author:** Esther Blanco-Paniagua; e–mail: eblap@unileon.es

ABSTRACT

The ATP-binding cassette transporter G2 (ABCG2) is a membrane transporter that conditions pharmacokinetics, systemic exposure, and milk secretion of drugs, natural and food-derived compounds, including gut-derived metabolites. *p*-Cresyl sulfate (*p*CS), a well-known uremic toxin, is the main metabolite of *p*-Cresol (*p*C), produced from dietary aromatic amino acids by gut microbiota. We aimed to characterize the *in vitro* and *in vivo* interaction of *p*CS with the ABCG2 transporter. Using MDCK–II cells overexpressing the transporter, we found that *p*CS is an *in vitro* substrate of ABCG2. Furthermore, using wild-type and Abcg2$^{-/-}$ mice, we showed that plasma $AUC_{0\text{-}240min}$ for Abcg2$^{-/-}$ was almost 1.6-fold higher than for wild-type mice. Regarding tissue distribution, the liver, kidney, small intestine, testis, and spleen from Abcg2$^{-/-}$ mice showed significantly higher *p*CS levels versus the wild-type group. Moreover, *p*CS accumulation in small intestine content retrieved from wild-type mice was 2-fold higher than in the Abcg2$^{-/-}$ group. Finally, we proved that Abcg2 also affects *p*CS secretion into milk, with a more than 3-fold higher accumulation in milk and almost 6-fold higher milk-to-plasma ratio of wild-type versus Abcg2$^{-/-}$ mice. Overall, our results disclose that Abcg2 significantly affects plasma levels, biodistribution and milk secretion of *p*CS, thereby modulating its biological activity.

Keywords: *p*-cresyl sulfate, ABCG2, milk secretion, plasma levels, tissue distribution, transepithelial transport assays.

Abbreviations: AB, apical to basolateral; ABCG2, ATP-binding cassette transporter G2; AUC, area under the plasma concentration-time curve; BA,

basolateral to apical; bABCG2, bovine ABCG2; BCRP, breast cancer resistance protein; C_{max}, maximum plasma concentration; DMEM, Dulbecco's modified Eagle's medium; HEPES, 4-(2-hydroxyethyl)−1-piperazineethanesulphonic acid; hABCG2, human ABCG2; IQ, 2-amino-3-methylimidazo[4,5-*f*]quinoline; LOD, limit of detection; LOQ, limit of quantification; mAbcg2, murine Abcg2; MDCK-II, Madin-Darby canine kidney; oABCG2, ovine ABCG2; *p*C, *p*-Cresol; *p*CG, *p*-cresyl glucuronide; *p*CS, *p*-cresyl sulfate; Phe, phenylalanine; PhIP, 2-amino-1-methyl-6-phenylimidazo[4,5-*b*]pyridine; SNPs, single-nucleotide polymorphisms; SULT1A1, sulfotransferase 1A1; Tyr, tyrosine; UPLC, ultra-performance liquid chromatography.

INTRODUCTION

Gut microbiota plays an important role in regulating the production of a plethora of microbial metabolites with key functions in the host's metabolic regulation [1]. *p*-Cresyl sulfate (*p*CS), the most well-studied and damaging protein-bound uremic toxin [2,3], is one of the aforementioned metabolites, which is synthesized through a multistep process involving both gut microbial and host factors [4,5], as will be explained below.

Dietary aromatic amino acids tyrosine and phenylalanine are converted into *p*-cresol (*p*C) [6–8], predominantly in the distal part of the colon through bacterial fermentation [9–11]. Within the human gut microbiota, specific bacterial families, such as *Fusobacteriaceae*, *Enterobacteriaceae*, *Clostridiaceae*, and *Coriobacteriaceae*, are recognized as strong *p*C producers. *p*C undergoes sulfation to yield *p*CS by the sulfotransferase 1A1 (SULT1A1), highly expressed in enterocytes of the colonic mucosa [12], prior to release into the portal vein [1,13]. Unmetabolized *p*C can also be transformed into *p*CS in the liver [14,15] by SULT1A1, which is highly abundant in hepatocytes as well [12] (Fig. 1). Although *p*C is mainly converted into its sulfated metabolite, a small fraction is glucuronated into *p*-cresyl glucuronide (*p*CG) [16,17] by host epithelial UDP-glucuronosyltransferases 4. Consequently, changes in diet composition, as well as gut microbiota, may interfere with *p*CS production [14,18,19]. Eventually, *p*CS is cleared by the kidney, ending up in the urine, making it a urinary marker of renal disease progression [6,20,21] (Fig. 1).

Regarding biological effects, accumulation of *p*CS under renal impairment conditions [22] causes toxicity in several tissues, primarily affecting the renal system, as well as the liver. Mainly, pro-apoptotic and proinflammatory effects

have been described [23–28], along with an induction of oxidative stress [29]. Besides, toxic effects in the cardiovascular system have also been reported [20,30–37].

Furthermore, *p*CS is the predominant alkylphenol in ruminant milk [38,39]. Recently, Potts and Peterson have described *p*CS as a small molecule whose presence in bovine milk may alter its somatosensory attributes [40]. This fact, coupled with the potential presence of the enzyme arylsulfatase in milk, which transforms *p*CS into *p*C [41], associated with off-flavors described as barnyard and cowshed in milk [42,43], may cause an impairment of the somatosensorial properties of milk, which is directly linked to milk quality, rendering it unacceptable to consumers [44,45].

Knowledge of the factors influencing bioavailability, tissue distribution, and secretion into milk of *p*CS is of particular relevance, considering the toxic effects associated with this molecule and the decline in milk quality related to the presence of this metabolite in that biological fluid.

ABCG2, also known as breast cancer resistance protein (BCRP), is a membrane transporter expressed in the apical membrane of cells of several tissues, including the jejunum, liver, and kidney [46]; biological barriers, such as the blood-brain, blood-testis and blood-placental barriers [47,48]; and the alveolar epithelial cells of the lactating mammary gland [49]. It acts as an efflux pump, extruding drugs as well as natural and endogenous compounds from the cells, thereby affecting their absorption, distribution, and elimination [50–52]. Consequently, ABCG2 influences the pharmacokinetics and systemic exposure, reducing plasma levels of its substrates [47]. Notably, being upregulated during

lactation [53], it is the only ABC transporter involved in the secretion of its substrates into milk [49].

Previous studies using membrane vesicles expressing the human ABCG2 variant suggested that *p*CS is an *in vitro* substrate of this transporter [54]. Notwithstanding, vectorial transport and *in vivo* interactions remain unknown. Accordingly, this study aimed to assess the *in vitro* interaction of *p*CS with different species variants of ABCG2, as well as to evaluate the role of this transporter in the pharmacokinetics, tissue distribution, and milk secretion of *p*CS, in order to correlate *in vitro* and *in vivo* outcomes.

RESULTS

In Vitro Transport of p-cresyl sulfate and p-cresol

The polarized cell line Madin-Darby canine kidney (MDCK-II) was used to determine the role of ABCG2 in the *in vitro* transport of *p*CS. Parental cell line and its subclones transduced with the murine Abcg2 (mAbcg2) and human, ovine, and bovine ABCG2 (hABCG2, oABCG2 and bABCG2, respectively) were grown to form confluent monolayers, which were used to evaluate the vectorial transport of *p*CS (Fig. 2). In addition, relative efflux ratios were calculated (Table 1). A similar transport pattern was observed in the parental MDCK-II cell line, with equal apical to basolateral (AB) and basolateral to apical (BA) vectorial translocation (Fig. 2a), which is reflected in the relative efflux transport ratio (BA/AB) at 4 h, 1.04 ± 0.10 (Table 1). In contrast, polarized MDCK-II cells overexpressing ABCG2 exhibited a markedly enhanced BA transport and a significantly reduced AB transport (Fig. 2c, e, g, i) when compared with parental cells. This resulted in significantly higher relative efflux transport ratios at 4 h in

comparison with the parental cell line (3.83 ± 0.31 for murine Abcg2, $p < 0.001$; 2.31 ± 0.28 for human ABCG2, $p = 0.003$; 15.47 ± 4.79 for ovine ABCG2, $p = 0.009$; and 2.21 ± 0.43 for bovine ABCG2, $p = 0.012$) (Table 1).

The specificity of ABCG2-mediated transport was checked using Ko143, the specific inhibitor of ABCG2 [55]. In all subclones, ABCG2-mediated transport was completely inhibited (Fig. 2d, f, h, j), and similar relative efflux transport ratios between parental and transduced cells were obtained (Table 1). These findings indicate that *p*CS is an effective *in vitro* substrate of ABCG2.

In the case of *p*C, no difference was observed in vectorial translocation between AB and BA in parental and mAbcg2 transduced cells, with an efflux ratio at 4h of (0.96 ± 0.05 for MDCK-II cells vs. 0.99 ± 0.16 for murine Abcg2 transduced cells, n = 4-5, $p = 0.740$), indicating that *p*C is not an Abcg2 substrate.

Plasma Pharmacokinetics Assays in Wild-Type and Abcg2$^{-/-}$ Male Mice

Plasma *p*CS concentrations were measured in wild-type and Abcg2$^{-/-}$ male mice and expressed as a function of time following administration of *p*C, the parental molecule, for the purpose of assessing whether *in vitro* ABCG2-mediated transport of *p*CS is mirrored *in vivo*. After oral dosing of *p*C, the maximum plasma concentration (C_{max}) of *p*CS was detected at the first sampling time point (30 min) in both groups of mice (Fig. 3), being in Abcg2$^{-/-}$ mice more than 2.5-fold higher than in the wild-type counterparts (2.69 ± 0.61 µg/mL vs. 1.06 ± 0.23 µg/mL; $p < 0.001$). Statistically significant differences were also observed at 90 min (0.48 ± 0.19 µg/mL in wild-type mice vs. 1.07 ± 0.30 µg/mL in Abcg2$^{-/-}$ mice; $p = 0.011$) and 120 min post-administration (0.47 ± 0.08 µg/mL in wild-type mice vs. 0.68 ± 0.17 µg/mL in Abcg2$^{-/-}$ mice; $p = 0.047$). *p*CS plasma

levels obtained at the 240-minute time point were below the limit of quantification (LOQ), so they were not included in Fig. 3.

The estimated area under the plasma concentration-time curve (AUC) corroborated significant differences in plasma concentration-time profiles between both groups of mice. The AUC parameter from 0 min to 240 min post-administration for Abcg2$^{-/-}$ mice was almost 1.6-fold higher than in the wild-type counterparts (3.04 ± 0.09 µg·h/mL vs. 1.91 ± 0.15 µg·h/mL; $p = 0.022$).

Our findings further corroborate the fact that Abcg2 modulates the plasma pharmacokinetic profile of *p*CS.

Tissue Distribution Assays in Wild-Type and Abcg2$^{-/-}$ Male Mice

*p*CS concentration was analyzed in a range of tissues, including liver, kidney, small intestine, small intestine content, spleen, brain, testis, and heart, 2 h after administration of a single oral dose of 10 mg/kg *p*C (Fig. 4).

*p*CS was detected in all tissues analyzed. When Abcg2 was lacking, tissue accumulation of *p*CS in almost all organs studied was significantly higher in comparison with wild-type mice. Notably, the Abcg2$^{-/-}$ group of mice showed a 2.8-fold higher accumulation in liver (4.84 ± 1.73 µg/g in Abcg2$^{-/-}$ vs. 1.69 ± 0.56 µg/g in wild-type, $p = 0.025$), a 1.5-fold higher concentration in kidney (16.39 ± 4.27 µg/g in Abcg2$^{-/-}$ vs. 10.60 ± 1.43 µg/g in wild-type, $p = 0.021$), almost 2.3-fold higher levels in small intestine (15.23 ± 6.90 µg/g in Abcg2$^{-/-}$ vs. 6.63 ± 2.76 µg/g in wild-type, $p = 0.042$), a 2.6-fold higher accumulation in spleen (14.07 ± 4.40 µg/g in Abcg2$^{-/-}$ vs. 5.38 ± 4.21 µg/g in wild-type, $p = 0.009$) and an almost 2-fold higher concentration in testis (13.49 ± 1.43 µg/g in Abcg2$^{-/-}$ vs. 7.02 ± 0.40 µg/g in wild-type, $p = 0.030$).

Additionally, the small intestine content retrieved from wild-type mice showed a 2.2-fold higher accumulation in comparison with Abcg2$^{-/-}$ mice (5.26 ± 2.41 µg/g in wild-type vs. 2.41 ± 0.79 µg/g in Abcg2$^{-/-}$, $p = 0.037$). These results indicate that Abcg2 mediates *p*CS excretion into the intestinal lumen, thereby contributing to its elimination.

The observed differences in tissue distribution substantiate that Abcg2 influences *p*CS biodistribution.

Milk Secretion Assays in Wild-Type and Abcg2$^{-/-}$ Lactating Female Mice

To assess whether Abcg2 contributes to *p*CS secretion into milk, the parental molecule was orally given at 10 mg/kg to lactating wild-type and Abcg2$^{-/-}$ female mice. Blood and milk samples were collected 2 h after administration (Fig. 5).

*p*CS plasma concentrations (Fig. 5a) were similar in the two groups of mice (0.73 ± 0.40 µg/mL in Abcg2$^{-/-}$ vs. 0.46 ± 0.27 µg/mL in wild-type, $p = 0.053$). By contrast, milk from the wild-type mice (Fig. 5b) showed a 3.2-fold higher accumulation compared to their Abcg2$^{-/-}$ counterparts (1.47 ± 0.73 µg/mL in wild-type vs. 0.46 ± 0.21 µg/mL in Abcg2$^{-/-}$, $p = 0.003$). Furthermore, the milk-to-plasma ratio of *p*CS (Fig. 5c) in wild-type mice was almost 6-fold higher than in Abcg2$^{-/-}$ mice (4.31 ± 3.29 vs. 0.74 ± 0.40; $p = 0.012$).

Based on the aforementioned data, we determine that Abcg2 is actively involved in the secretion of *p*CS into milk, providing strong evidence of its *in vivo* interaction with the transporter.

DISCUSSION

Alkylphenols represent key flavor-active compounds in dairy products, existing largely in conjugated forms within ruminant milk [38]. Of them, *p*C and its conjugates are the principal alkylphenols detected in ruminant milk, with the sulfated metabolite, *p*CS, as the predominant form [39]. Given its role in the somatosensory attributes of milk products [40], and its biological effects derived from its accumulation in the bloodstream and tissues as a consequence of being a uremic retention solute [56–58], it is of the utmost importance to study the pharmacokinetics and biodistribution of *p*CS and whether it is influenced by the presence of the efflux transporter ABCG2.

Accordingly, although previous studies have already suggested the active transport of *p*CS via transporters such as P-glycoprotein [59] and hABCG2 [54], this study shows for the first time the *in vitro* interaction of *p*CS with mAbcg2, oABCG2, and bABCG2 and confirms the *in vitro* interaction with hABCG2. Likewise, it provides first evidence of the impact of murine Abcg2 on plasma concentrations, systemic exposure, and milk secretion of *p*CS.

Regarding *in vitro* assays, *in vitro* transepithelial transport assays demonstrated that *p*CS is efficiently transported by all variants of ABCG2 (Fig. 2, Table 1), as well as other gut microbiota-derived compounds such as the ellagic acid-derived metabolite, urolithin A [60], and the lignan-derived metabolites enterodiol [61] and enterolactone [62]. These results differ from those observed for the parent compound (*p*C), which has not been identified as an *in vitro* substrate of ABCG2. Interactions with ABCG2 are strongly influenced by the physicochemical properties of molecules, with hydrophobicity playing a key role. In this case, sulfation of *p*C to form *p*CS increases not only its hydrophilicity, but also its topological surface area [63,64]. This physicochemical behavior has also

been reported for other compounds, such as albendazole [65,66] and thiabendazole [67], in which only the metabolites, rather than the parent compounds, function as *in vitro* substrates of ABCG2.

Differences observed between murine and human ABCG2-transduced subclones (Fig. 2, Table 1) were consistent with those reported for other gut-derived metabolites, such as enterodiol [61] and urolithin A [60], and for other endogenous ABCG2 well-known substrates, such as lumichrome [68] and riboflavin, its precursor [69], and 6-sulfatoxymelatonin, the main phase II metabolite of melatonin [70]. It should also be noted that, similar to human ABCG2-transduced subclones, cells transduced with bABCG2 exhibit lower transport ratios at 4 h than murine ABCG2-transduced subclones. In contrast, cells transduced with oABCG2 display markedly higher transport ratios compared to those transduced with other transporter variants (Table 1). These disparities were in line with those previously reported for the gut-derived metabolite, urolithin A [60]; for the hydroxylated melatonin metabolite, 6-hydroxymelatonin [70]; and for some drugs [67,71,72]. These divergences may reflect variations in the expression and in the affinity or selectivity of a species-specific transporter for the compound. However, we cannot rule out possible differences in transduction efficiency [73,74].

Results obtained for the human variant of the transporter are consistent with the ones previously reported, in which *in vitro* studies were carried out in membrane vesicles transduced with human ABCG2 [54]. Vesicular membrane transport models have been used since the 1950s to study the transport of substances across cell membranes. Nevertheless, they are structurally simpler than the polarized MDCK-II cells used in the current study [75], which more

closely reflect the physiological transport of potential substrates of ABCG2 [76], further reinforcing that *p*CS is an *in vitro* substrate of human ABCG2.

Regarding our positive outcomes with cells overexpressing the ruminant variants of the transporter, they support experiments conducted by Kilic *et al.* (2005) that confirmed the appearance of *p*CS in ovine and bovine milk without addressing the underlying excretion mechanism at that moment [39]. Studying the *in vitro* transport mediated by the ovine and bovine variants of ABCG2 allowed us to analyze its activity more exhaustively, paving the way for further research into the presence of *p*CS in milk mediated by ABCG2 and the consequences of its consumption.

Regarding *in vivo* assays, *p*CS concentrations were determined in plasma and several tissues of male wild-type and Abcg2$^{-/-}$ mice after the oral administration of *p*C, the precursor metabolite, at a dose of 10 mg/kg. Although *p*CS exhibits strong plasma protein binding [14,22,77], the plasma protein precipitation undertaken in the sample preparation enables measurement of its total plasma concentration.

After the sulfation of *p*C by SULT1A1, which is highly expressed in hepatocytes and enterocytes [12], as was previously noted, *p*CS was rapidly absorbed in both groups of mice. However, plasma concentrations remained higher in Abcg2$^{-/-}$ mice compared to the wild-type mice at 30 min, 90 min, and 120 min time points, resulting in increased systemic exposure in Abcg2$^{-/-}$ mice (Fig. 3), as evidenced by a higher $AUC_{0\text{-}240min}$ in that group of mice. Similarly, in the case of the antibacterial agent nitrofurantoin [76] and the anti-inflammatory drugs tolfenamic acid [78] and meloxicam [79], following oral administration, plasma levels of these compounds were higher in Abcg2$^{-/-}$ mice compared to

their wild-type counterparts. This supports the idea that Abcg2 contributes to *p*CS plasma bioavailability.

Concerning tissue distribution, *p*CS was demonstrated to be extensively distributed across multiple tissues (Fig. 4). With regards to the small intestine, likewise for other Abcg2 substrates such as melatonin [70] and the carcinogenic heterocyclic amines 2-amino-1-methyl-6- phenylimidazo[4,5-*b*]pyridine (PhIP) [80,81] and 2-amino-3-methylimidazo[4,5-*f*]quinoline (IQ) [82], higher concentrations of *p*CS were found in the intestine of the Abcg2$^{-/-}$ mice in comparison with their wild-type counterparts. In contrast, concentrations in the small intestine content retrieved from wild-type mice were higher than from Abcg2$^{-/-}$ mice. This indicates that Abcg2 may reduce *p*CS oral bioavailability by altering its intestinal absorption, as reflected by decreased concentrations in the enterocytes of the small intestine and elevated concentrations in the intestinal lumen of the wild-type mice.

In the kidney, the Abcg2$^{-/-}$ mice presented a 1.5-fold higher *p*CS concentration than the wild-type mice (Fig. 4). This suggests reduced renal elimination of this compound and its subsequent accumulation in the kidneys of knockout animals, supporting the fact that Abcg2 participates in the renal elimination of *p*CS, its main route of excretion [4,14,15]. The transporter Abcg2 also plays a key role in the urinary elimination of other sulfated metabolites [83], such as *trans*-resveratrol sulfate [84], enterolactone sulfate [85], 6-sulfatoxymelatonin [70], and indoxyl sulfate [86]. The fact that *p*CS is utilized as a urinary marker of renal disease progression [6,20,21], together with being a human *in vitro* substrate of ABCG2, may be of significance for human clinical applications, as well as in the case of 6-sulfatoxymelatonin [70]. As was stated

before, an accumulation of *p*CS has been associated with renal injury. Pro-apoptotic effects have been described for this molecule [23–25], along with the increase in the expression of cytokines and proinflammatory genes in renal tubular cells, the activation of the renin-angiotensin-aldosterone system and the TGF-β1 pathway, and the induction of epithelial-mesenchymal transitions, leading to renal fibrosis [26–28]. Besides, high levels of *p*CS lead to a decrease in Klotho expression, contributing in this way to the senescence of renal cells [87]. Alterations in the ABCG2 expression or functionality may condition renal distribution of its substrates, including *p*CS, which could have an impact on its effects [48,88], due to its role as an urinary marker, resulting in potential misinterpretations of the renal damage.

Additionally, a higher accumulation of *p*CS was observed in the liver and spleen of the Abcg2$^{-/-}$ mice when compared to the wild-type mice (Fig. 4). An impairment of the normal function of the liver [29,89] and the immune response [90,91] has been shown in the presence of clinically significant levels of *p*CS. In the liver, *p*CS induces oxidative stress, glutathione depletion, cellular necrosis, bile acid transport disorders, and apoptosis [29]; whereas it suppresses Th1-type cellular immune response [91], and although it induces macrophage activation, it hampers antigen processing, resulting in a compromised adaptive immune response [90].

Finally, no significant differences in *p*CS heart accumulation were found between Abcg2$^{-/-}$ and wild-type mice (Fig. 4). Similar *p*CS concentrations may be due to the inherently low expression of Abcg2 in cardiac tissue with respect to pharmacologically relevant tissues such as the liver, kidney, or the gastrointestinal tract, where Abcg2 is more highly expressed [92].

Taking these findings together, Abcg2, which is expressed on the apical membrane of cells of tissues and biological barriers and mediates the egress of its substrates from the cell [46-48], affects the accumulation of *p*CS in the liver, kidney, spleen, and testis after its oral administration. Consequently, Abcg2$^{-/-}$ mice exhibit a more elevated drug exposure compared with the wild-type group, potentially leading to increased toxicity. Alterations in Abcg2 activity may result in changes in these toxicological effects due to *p*CS.

In light of these results, Abcg2 has a meaningful impact on the pharmacokinetics and tissue distribution of *p*CS as the activity of the transporter may be reduced by many molecules, such as natural and dietary compounds comprising soy isoflavones [93,94] and flaxseed [95], the primary source of dietary lignans [96], both polyphenols [97], along with the concomitant administration of multiple drugs commonly used in the treatment of human diseases [98–101]. As well, genetic single-nucleotide polymorphisms (SNPs) could also give rise to a dysfunction of the transporter. This is the case of Q141K, which presents a significant incidence within the Asian population [102].

With respect to milk, the involvement of Abcg2 in the active secretion of *p*CS was also assessed after the oral administration of *p*C at a dose of 10 mg/kg to lactating wild-type and Abcg2$^{-/-}$ lactating mice.

Unlike in male mice, plasma levels of *p*CS in the female wild-type group were comparable to their Abcg2$^{-/-}$ counterparts, which may be due to the higher interindividual variability compared to male mice or to the more elevated Abcg2 expression and activity in the liver from male mice in comparison to female mice, as reported in previous studies [103]. Albeit the lack of significant differences in plasma concentrations between wild-type and Abcg2$^{-/-}$ female mice, *p*CS

concentrations in milk (Fig. 5b) were 3.2-fold higher in the wild-type group in comparison to the Abcg2$^{-/-}$ mice, as well as the milk-to-plasma ratio (Fig. 5c), being in the wild-type group of lactating mice almost 6-fold higher than in the Abcg2$^{-/-}$ lactating mice. These divergences in milk concentrations of *p*CS and milk-to-plasma ratio have also been observed for other gut microbial metabolites that are Abcg2 substrates, such as enterodiol [61] and enterolactone [61,62]. Moreover, the administration of other natural substrates likewise resulted in elevated concentrations of them in the milk of wild-type relative to Abcg2$^{-/-}$ mice, such as riboflavin [69] and its byproduct, lumichrome [68], melatonin and its metabolites [70], biotin [69], and bile acids [104]. Taken together, these findings indicate that Abcg2 plays a key role in the active secretion of *p*CS into milk, thereby influencing its milk concentration.

Any factor that could modify the expression or the activity of the ABCG2 transporter could have an impact on the concentration of ABCG2 substrates secreted into milk [49], as is the case for *p*CS, reported in this work. This metabolite is known to modify somatosensory flavor attributes in milk [40] and, in the presence of an arylsulfatase, could be transformed into *p*C [41], responsible for unpleasant barnyard [42,43] and cow-shed aroma in milk [41]. Thereby, alterations in the ABCG2 transporter could vary *p*CS milk concentrations, which may consequently influence milk quality.

The identification of ABCG2 as a key determinant in regulating levels of *p*CS in plasma, tissue, and milk, together with the impact of gene regulation (ABCG2) and environmental factors, including dietary modifications [105] and gut microbiota alterations [106,107], on *p*CS production and accumulation, underscores their potential clinical significance. **CONCLUSIONS**

Based on the above, we can conclude that the ABCG2 transporter interacts with the gut-derived metabolite *p*CS. This work shows for the first time that ABCG2 is clearly involved in the active *in vitro* transport of *p*CS by murine, human, ovine, and bovine variants. Moreover, *in vivo* experiments allowed us to demonstrate that Abcg2 affects pharmacokinetics, biodistribution, and secretion into milk of *p*CS. Thus, changes in ABCG2 expression or function may influence plasma and milk concentrations, along with tissue distribution of *p*CS, potentially affecting its biological effects.

METHODS

Chemicals

*p*CS, *p*C, and albendazole-2-amino sulfone were purchased from LGC Standards (Teddington, Middlesex, UK). Lucifer Yellow and Ko143 were acquired from ThermoFisher (Waltham, MA, USA) and Tocris (Bristol, UK). The buffer 4-(2-hydroxyethyl) −1-piperazineethanesulphonic acid (HEPES), utilized in *in vitro* assays, anthranilic acid, and the charcoal activated used to prepare the milk matrix blanks were purchased from Sigma Aldrich (St. Louis, MO, USA). For *in vivo* assays, isoflurane (Isovet®) was obtained from B. Braun VetCare (Barcelona, Spain), oxytocin (Falcipart) from SYVA (León, Spain) and heparin (ROVI®) from Laboratorios Farmacéuticos ROVI, S.A. (Madrid, Spain).

Cell Cultures

The polarized cell line Madin-Darby canine kidney (MDCK-II) and its murine Abcg2 and human ABCG2 transduced subclones, previously generated [81,108] and provided by Dr. A. H. Schinkel from the Netherlands Cancer Institute (Amsterdam, The Netherlands), were used for *in vitro* studies. Transduced

subclones with the ovine and bovine variants of ABCG2 were previously generated by our research group [109,110]. Cell culture conditions have been previously described [109]. Concisely, cells were cultured at 37 °C in an atmosphere with 5% CO_2 in Dulbecco's modified Eagle's medium (DMEM) supplemented with GlutaMAX™ (Life Technologies Limited, Paisley, UK), penicillin (50 units/mL) and streptomycin (50 µg/mL) (Life Technologies Corporation, Grand Island, NY, USA) and 10% (v/v) fetal bovine serum (MP Biomedicals, Solon, OH, USA. Cells were trypsinized when a subconfluent state was reached for subculturing.

Transepithelial transport assays

Transepithelial transport assays were carried out as previously described [76], with slight modifications. Cells were seeded at 1.0 x 10^6 cells/well as a monolayer on microporous membrane filters (3.0 µm pore size, 24 mm diameter; Transwell® 3414; Costar, Corning, NY). Cells were grown for three days, and culture medium was replaced daily.

At the beginning and the end of the assay, monolayer tightness was checked using Millicell®ERS 3.0 Digital Voltohmmeter (Merck Millipore, Burlington, MA, USA). Likewise, monolayer confluence was tested at the end of the experiment via Lucifer Yellow permeability assay [111]. Transport proficiency was constantly checked by testing a typical ABCG2 substrate (nitrofurantoin 10 µM) [76].

Two hours before the start of the assay, medium at both the apical and basolateral side of the monolayer was replaced with 2 mL of prewarmed Hanks' balanced salt solution (Sigma-Aldrich) supplemented with HEPES (25 mM), the transport medium, either with or without the inhibitor Ko143 (1 µM) [68,76], to

verify the specificity of ABCG2 on the potential transport. The experiment began (t = 0 h) by replacing the medium of the apical or basal compartments with fresh transport medium containing 10 µM *p*CS, either with or without inhibitor, or 10 µM *p*C. Cells were incubated at 37°C in 5% CO_2 and 100 µL aliquots were collected at 1, 2 and 3 h on the opposite side from where *p*CS or *p*C had been added. This volume was replaced with fresh transport medium. Finally, 600 µL aliquots were taken at 4h time from both compartments of each well. All samples were stored at −20°C until being analyzed by ultra-performance liquid chromatography (UPLC), as described below.

The appearance of the compounds studied in the opposite compartment is presented as the fraction of total compound added at the beginning of the experiment and expressed as percentage. The relative efflux transport ratio was calculated as the basal to apical directed transport percentage divided by the apical to basal directed transport percentage at 4 h.

Animals

Animals were housed and handled in accordance with institutional and ARRIVE guidelines and European legislation (Directive 2010/63/EU). Experimental procedures were conducted in compliance with relevant guidelines and regulations and were approved by the Animal Care and Use Committee of the University of León and the Junta de Castilla y León (ULE_009_2023). Abcg2$^{-/-}$ and wild-type mice were used, all of >99% FVB/N genetic background, generated and kindly supplied by Dr. A. H. Schinkel (The Netherlands Cancer Institute) [112]. All animals, aged from 9 to 14 weeks and weighing 20-36 g, were kept in a temperature-controlled environment with a 12:12 light/dark cycle and received a standard diet and water *ad libitum*.

Plasma and tissue distribution

For *in vivo* assays, male mice were lightly anesthetized with isoflurane and administered an oral dose of *p*C, the parental molecule, via oral gavage. A dose of 10 mg/kg was selected, as it represents the minimum required to detect the sulfated metabolite in biological samples using the chromatographic method described in the *Ultra-performance liquid chromatographic analysis* section. For these administrations, *p*C dissolved in saline solution was dosed at 300 µl per 30 g of body weight.

Blood samples were collected at different time points (30, 45, 60, 90, 120, 150, 180 and 240 min). Each mouse contributed two samples under isoflurane anesthesia (retro-orbital and cardiac puncture at different time points). Organs were harvested at the 120-minute time point. All animals were euthanized by cervical dislocation at the end of the experimental procedure. Heparinized blood samples were centrifuged immediately at 3000 g for 15 min [68]. Plasma and organs were stored at −20°C until UPLC analysis. Four to six animals were used for each time point. The AUC was estimated as a pooled parameter using the linear trapezoidal rule, since only two samples were collected from each individual animal.

Milk secretion experiments

Milk secretion experiments were performed using female mice mated with males. Females were separated from males upon detection of a vaginal plug or after five days of cohabitation. Pregnant females were housed individually, and the day of pup birth was recorded. Experiments were conducted between days 10 and 14 postpartum. Four hours prior to the start of the experiment, pups were separated from their mothers. *p*C at a dose of 10 mg/kg and dissolved in saline

solution, was orally administered to lactating wild-type and Abcg2$^{-/-}$ female mice, at 300 µL per 30 g of body weight. Milk secretion was stimulated by subcutaneous injection of oxytocin (200 µL of a 1 IU/mL solution) into lactating mice 10 min before sample collection. Subsequently, 2 h after *p*C administration, blood and milk samples were collected under isoflurane anesthesia by retro-orbital plexus puncture and gentle nipple pinching using capillaries, respectively. At the end of the experiment, animals were euthanized by cervical dislocation. Heparinized blood samples were centrifuged immediately at 3000 g for 15 min to collect plasma. Milk and plasma were also kept at −20°C until UPLC analysis. Nine to eleven animals were used for each group.

Sample preparation

Tissue samples were homogenized with a solution of potassium phosphate monobasic at a concentration of 0.3M with an adjusted pH 3.2; 1 mL of solution per 0.1 g of organ was used. A volume of 10 µL of the appropriate internal standard solution was added to each 100 µL of milk, plasma, or tissue homogenate. Anthranilic acid (10 µg/mL) served as the internal standard for plasma and tissue samples, while albendazole-2-aminosulfone (5 µg/mL) was used for milk samples. In addition, 600 µL of acetonitrile was added to precipitate proteins. After 10 min of being horizontally vortexed, samples were centrifuged at 14,000 g for 15 min at 4°C. Supernatants were evaporated to dryness at 40°C under a stream of nitrogen. Samples were reconstituted in 100 µL of cold methanol and injected into the UPLC system. However, samples for *in vitro* assays were directly injected into the UPLC system.

Ultra-performance liquid chromatographic analysis

Sample analysis was performed on a Waters ACQUITY UPLC H-class system coupled with a UV photodiode array detector. Chromatographic separation was undertaken on an Acquity UPLC BEH C18 column (1.7 µm particle size, 2.1 x 50 mm, 130 Å, Waters Corporation, Milford, MA, USA) maintained at 40°C. The binary mobile phase consisted of 0.1% formic acid aqueous solution (solvent A) and acetonitrile with 0.1% formic acid (solvent B) as the organic phase. Chromatography was performed using a flow rate of 0.7mL/min with the following linear gradient: solvent B at 5% (0-3.75 min), increased to 80% (3.75-3.80 min), increased to 95% (3.80-5.40 min) decreased to 20% (5.40-5.70 min) and held at 20% (5.70-13 min). For *p*C, the gradient started at 15% of solvent B, while the remaining conditions were identical. The UV absorbance for *p*CS was measured at 218 nm and for *p*C at 220 nm, and samples were maintained at 4°C throughout the analysis.

For proper quantification of *p*CS levels in milk samples, a milk analyte-free matrix was prepared as previously described with minor modifications [113]. A portion of 5 g of milk powder was resuspended in 50 mL of distilled water by vortexing until complete homogenization. Following this, 100 mg of activated charcoal was added into 1 mL of milk solution. The mixture was horizontally vortexed for 2 h at room temperature and centrifuged at 4000g for 20 minutes at 4ºC. The supernatant was transferred to clean eppendorf tubes and centrifuged again at 14000 g for 20 minutes at 4ºC. The supernatant was transferred again to clean eppendorf tubes and kept at −20°C until use.

Standard samples of *p*CS were prepared in the appropriate analyte-free matrix to generate a defined concentration range between 0.0195–10 µg/mL for culture, 0.156-20 µg/mL for plasma and tissue samples, and 0.156–10 µg/mL for

milk samples. Coefficients of correlation for culture and milk samples were above 0.98, whereas in plasma samples they ranged between 0.95 and 0.99, and in tissue samples between 0.91 and 0.99. Similarly, standard solutions of *p*C were prepared to obtain a concentration range of 0.0195–10 µg/mL for culture samples, showing correlation coefficients above 0.99.

The LOQ and limit of detection (LOD) were calculated as described by Taverniers et al. [114]. In the case of *p*CS, LOQ was 0.009 µg/mL and LOD 0.004 µg/mL for cell culture samples; LOQ was 0.110 µg/mL and LOD 0.057 µg/mL for plasma samples; LOQ was 0.138 µg/mL and LOD 0.070 µg/mL for milk samples, and for tissues, LOQ was 0.074-0.296 µg/mL and LOD 0.035–0.141 µg/mL. Regarding *p*C, LOQ was 0.005 µg/mL and LOD 0.004 µg/mL for culture samples.

Statistical analysis

Statistical analyses were conducted using SPSS Statistics software (v. 29.0; IBM, Armonk, NY, USA). Data normality was assessed with the Shapiro-Wilk test. Comparisons between groups were performed using a two-tailed unpaired Student's T-test for normally distributed data or the Mann-Whitney U test for non-normally distributed data. Differences were considered statistically significant at $p \leq 0.05$.

DATA AVAILABILITY STATEMENT

The datasets used in this study are available in online repositories and can be found at the following link: https://open.scayle.es/dataset/millan-garcia_2026.

FUNDING

The authors declare that financial support was received for the research, authorship and/or publication of this article. This work was supported by the research projects PID2021-125660OB-I00 and PID2024-161728OB-I00 (MCIN/AEI/10.13039/501100011033/FEDER “Una manera de hacer Europa”) and by predoctoral grants (FPU23/00153 grant to A.M.-G.) from the Spanish Ministry of Education, Culture and Sport.

REFERENCES

1. Toft, P. B. *et al.* Microbial metabolite p-cresol inhibits gut hormone expression and regulates small intestinal transit in mice. *Front. Endocrinol. (Lausanne).* **14**, 1200391 (2023).
2. Vanholder, R., Pletinck, A., Schepers, E. & Glorieux, G. Biochemical and clinical impact of organic uremic retention solutes: A comprehensive update. *Toxins (Basel).* **10**, 1–57 (2018).
3. Du, Y. *et al.* Dietary influences on urinary tract infections: unraveling the gut microbiota connection. *Food Funct.* **15**, 10099–10109 (2024).
4. Graboski, A. L. & Redinbo, M. R. Gut-Derived Protein-Bound Uremic Toxins. *Toxins (Basel).* **12**, 590 (2020).
5. De Almeida Alvarenga, L. *et al.* Cranberries-potential benefits in patients with chronic kidney disease. *Food Funct.* **10**, 3103–3112 (2019).
6. Gryp, T., Vanholder, R., Vaneechoutte, M. & Glorieux, G. p -Cresyl Sulfate. *Toxins (Basel).* **9**, 52 (2017).
7. Wikoff, W. R. *et al.* Metabolomics analysis reveals large effects of gut microflora on mammalian blood metabolites. *Proc. Natl. Acad. Sci. U.S.A.* **106**, 3698–3703 (2009).
8. Ye, X. *et al.* Dual Role of Indoles Derived From Intestinal Microbiota on Human Health. *Front. Immunol.* **13**, 903526 (2022).
9. Smith, E. A. & Macfarlane, G. T. Enumeration of human colonie bacteria

producing phenolic and indolic compounds : Effects of pH, carbohydrate availability and retention time on dissimilatory aromatic amino acid metabolism. *J. Appl. Bacteriol.* **81**, 288–302 (1996).

10. Smith, E. A. & Macfarlane, G. T. Dissimilatory amino acid metabolism in human colonic bacteria. *Anaerobe* **3**, 327–337 (1997).

11. Renaldi, R., Wiguna, T., Persico, A. M. & Tanra, A. J. p-Cresol and p-Cresyl Sulphate Boost Oxidative Stress: A Systematic Review of Recent Evidence. *Basic Clin. Pharmacol. Toxicol.* **137**, e70065 (2025).

12. Teubner, W., Meinl, W., Florian, S., Kretzschmar, M. & Glatt, H. Identification and localization of soluble sulfotransferases in the human gastrointestinal tract. *Biochem. J.* **404**, 207–215 (2007).

13. Aronov, P. A. *et al.* Colonic contribution to uremic solutes. *J. Am. Soc. Nephrol.* **22**, 1769–1776 (2011).

14. Blachier, F. & Andriamihaja, M. Effects of the L-tyrosine- derived bacterial metabolite p-cresol on colonic and peripheral cells. *Amino Acids* **54**, 325–338 (2022).

15. Spicher, P. *et al.* Transporter-Mediated Interactions Between Uremic Toxins and Drugs: A Hidden Driver of Toxicity in Chronic Kidney Disease. *Int. J. Mol. Sci.* **26**, 6328 (2025).

16. Poesen, R. *et al.* Metabolism, protein binding, and renal clearance of microbiota-derived p-cresol in patients with CKD. *Clin. J. Am. Soc. Nephrol.* **11**, 1136–1144 (2016).

17. de Loor, H., Bammens, B., Evenepoel, P., De Preter, V. & Verbeke, K. Gas Chromatographic–Mass Spectrometric Analysis for Measurement of p-Cresol and Its Conjugated Metabo- lites in Uremic and Normal Serum. *Clin. Chem.* **51**, 1533–1535 (2005).

18. Blachier, F. *et al.* High-protein diets for weight management: Interactions with the intestinal microbiota and consequences for gut health. A position paper by the my new gut study group. *Clin. Nutr.* **38**, 1012–1022 (2019).

19. Beaumont, M. *et al.* Quantity and source of dietary protein influence metabolite production by gut microbiota and rectal mucosa gene expression: A randomized, parallel, double-blind trial in overweight humans. *Am. J. Clin. Nutr.* **106**, 1005–1019 (2017).

20. Koppe, L. *et al.* p-Cresyl sulfate promotes insulin resistance associated with CKD. *J. Am. Soc. Nephrol.* **24**, 88–99 (2013).

21. Vanholder, R., Schepers, E., Pletinck, A., Nagler, E. V & Glorieux, G. The Uremic Toxicity of Indoxyl Sulfate and p-Cresyl Sulfate : A Systematic Review. *J Am Soc Nephrol* **25**, 1897–1907 (2014).

22. André, C., Bodeau, S., Kamel, S., Bennis, Y. & Caillard, P. The AKI-to-CKD Transition: The Role of Uremic Toxins. *Int. J. Mol. Sci.* **24**, 16152 (2023).

23. Bammens, B., Evenepoel, P., Verbeke, K. & Vanrenterghem, Y. Removal of middle molecules and protein-bound solutes by peritoneal dialysis and

relation with uremic symptoms. *Kidney Int.* **64**, 2238–2243 (2003).

24. Mozar, A. *et al.* Uremic Toxin Indoxyl Sulfate Inhibits Human Vascular Smooth Muscle Cell Proliferation. *Ther. Apher. Dial.* **15**, 135–139 (2011).

25. Neirynck, N. *et al.* An update on uremic toxins. *Int. Urol. Nephrol.* **45**, 139–150 (2013).

26. Sun, C. Y., Chang, S. C. & Wu, M. S. Suppression of Klotho expression by protein-bound uremic toxins is associated with increased DNA methyltransferase expression and DNA hypermethylation. *Kidney Int.* **81**, 640–650 (2012).

27. Sun, C. Y., Chang, S. C. & Wu, M. S. Uremic toxins induce kidney fibrosis by activating intrarenal renin-angiotensin-aldosterone system associated epithelial-to-mesenchymal transition. *PLoS One* **7**, e34026 (2012).

28. Sun, C. Y., Hsu, H. H. & Wu, M. S. P-Cresol sulfate and indoxyl sulfate induce similar cellular inflammatory gene expressions in cultured proximal renal tubular cells. *Nephrol. Dial. Transplant.* **28**, 70–78 (2013).

29. Deng, M. *et al.* Short-Chain Fatty Acids Alleviate Hepatocyte Apoptosis Induced by Gut-Derived Protein-Bound Uremic Toxins. *Front. Nutr.* **8**, 756730 (2021).

30. Meijers, B. K. I. *et al.* The Uremic Retention Solute p-Cresyl Sulfate and Markers of Endothelial Damage. *Am. J. Kidney Dis.* **54**, 891–901 (2009).

31. Pletinck, A. *et al.* Protein-bound uremic toxins stimulate crosstalk between leukocytes and vessel wall. *J. Am. Soc. Nephrol.* **24**, 1981–1994 (2013).

32. Gross, P. *et al.* Para-cresyl sulfate acutely impairs vascular reactivity and induces vascular remodeling. *J. Cell. Physiol.* **230**, 2927–2935 (2015).

33. Guerrero, F. *et al.* Role of endothelial microvesicles released by p-cresol on endothelial dysfunction. *Sci. Rep.* **10**, 10657 (2020).

34. Mair, R. D., Sirich, T. L. & Meyer, T. W. Uremic toxin clearance and cardiovascular toxicities. *Toxins (Basel).* **10**, 226 (2018).

35. Falconi, C. A. *et al.* Uremic Toxins: An Alarming Danger Concerning the Cardiovascular System. *Front. Physiol.* **12**, 686249 (2021).

36. Velasquez, M. T., Centron, P., Barrows, I., Dwivedi, R. & Raj, D. S. Gut microbiota and cardiovascular uremic toxicities. *Toxins (Basel).* **10**, 287 (2018).

37. Han, H. *et al.* P-cresyl sulfate aggravates cardiac dysfunction associated with chronic kidney disease by enhancing apoptosis of cardiomyocytes. *J. Am. Heart Assoc.* **4**, e001852 (2015).

38. Lopez, V. & Lindsay, R. C. Metabolic Conjugates as Precursors for Characterizing Flavor Compounds in Ruminant Milks. *J. Agric. Food Chem.* **41**, 446–454 (1993).

39. Kilic, M. & Lindsay, R. C. Distribution of conjugates of alkylphenols in milk

from different ruminant species. *J. Dairy Sci.* **88**, 7–12 (2005).

40. Potts, D. M. & Peterson, D. G. Identification of small molecule flavor compounds that contribute to the somatosensory attributes of bovine milk products. *Food Chem.* **294**, 27–34 (2019).

41. Stressler, T., Leisibach, D. & Lutz-wahl, S. Homologous expression and biochemical characterization of the arylsulfatase from Kluyveromyces lactis and its relevance in milk processing. *Appl. Microbiol. Biotechnol.* **100**, 5401–5414 (2016).

42. Clarke, H. J. *et al.* Dietary compounds influencing the sensorial, volatile and phytochemical properties of bovine milk. *Molecules* **25**, 26 (2020).

43. Faulkner, H. *et al.* Effect of different forage types on the volatile and sensory properties of bovine milk. *J. Dairy Sci.* **101**, 1034–1047 (2018).

44. Min, D. B. & Boff, J. M. Chemistry and reaction of singlet oxygen in foods. *Compr. Rev. Food Sci. Food Saf.* **1**, 58–72 (2002).

45. Keim, J. P. *et al.* Milk production responses, rumen fermentation, and blood metabolites of dairy cows fed increasing concentrations of forage rape (Brassica napus ssp. Biennis). *J. Dairy Sci.* **103**, 9054–9066 (2020).

46. Hilgendorf, C. *et al.* Expression of Thirty-six Drug Transporter Genes in Human. *Basic Clin. Pharmacol. Toxicol.* **35**, 1333–1340 (2007).

47. Vlaming, M. L. H., Lagas, J. S. & Schinkel, A. H. Physiological and pharmacological roles of ABCG2 (BCRP): Recent findings in Abcg2 knockout mice. *Adv. Drug Deliv. Rev.* **61**, 14–25 (2009).

48. Horsey, A. J., Cox, M. H., Sarwat, S. & Kerr, I. D. The multidrug transporter ABCG2: still more questions than answers. *Biochem. Soc. Trans.* **44**, 824–830 (2016).

49. García-Lino, A. M., Álvarez-Fernández, I., Blanco-Paniagua, E., Merino, G. & Álvarez, A. I. Transporters in the Mammary gland—contribution to presence of nutrients and drugs into milk. *Nutrients* **11**, 2372 (2019).

50. Kukal, S. *et al.* Multidrug efflux transporter ABCG2: expression and regulation. *Cell. Mol. Life Sci.* **78**, 6887–6939 (2021).

51. Qi, X., Chen, H., Guan, K., Wang, R. & Ma, Y. Anti-hyperuricemic and nephroprotective effects of whey protein hydrolysate in potassium oxonate induced hyperuricemic rats. *J. Sci. Food Agric.* **101**, 4916–4924 (2021).

52. Ganguly, S. *et al.* Metabolomic and transcriptomic analysis reveals endogenous substrates and metabolic adaptation in rats lacking Abcg2 and Abcb1a transporters. *PLoS One* **16**, e0253852 (2021).

53. Beers, J. L., Hebert, M. F. & Wang, J. Transporters and drug secretion into human breast milk. *Expert Opin. Drug Metab. Toxicol.* **21**, 409–428 (2025).

54. Mutsaers, H. A. M. *et al.* Proximal tubular efflux transporters involved in renal excretion of p-cresyl sulfate and p-cresyl glucuronide: Implications for chronic kidney disease pathophysiology. *Toxicol. Vitr.* **29**, 1868–1877

(2015).

55. Allen, J. D. *et al.* Potent and Specific Inhibition of the Breast Cancer Resistance Protein Multidrug Transporter in Vitro and in Mouse Intestine by a Novel Analogue of Fumitremorgin C 1. *Mol. Cancer Ther.* **1**, 417–425 (2002).

56. Duranton, F. *et al.* Normal and pathologic concentrations of uremic toxins. *J. Am. Soc. Nephrol.* **23**, 1258–1270 (2012).

57. Vanholder, R. *et al.* Review on uremic toxins: Classification, concentration, and interindividual variability. *Kidney Int.* **63**, 1934–1943 (2003).

58. Vanholder, R., Glorieux, G., De Smet, R. & Lameire, N. New insights in uremic toxins. *Kidney Int. Suppl.* **63**, S6–S10 (2003).

59. Jourde-Chiche, N. & Burtey, S. Accumulation of protein-bound uremic toxins: the kidney remains the leading culprit in the gut-liver-kidney axis. *Kidney Int.* **97**, 1102–1104 (2020).

60. González-Sarrías, A. *et al.* The Gut Microbiota Ellagic Acid-Derived Metabolite Urolithin A and Its Sulfate Conjugate Are Substrates For The Drug Efflux Transporter Breast Cancer Resistance Protein (ABCG2/BCRP). *J. Agric. Food Chem.* **61**, 4352–4359 (2013).

61. García-Mateos, D. *et al.* The Breast Cancer Resistance Protein (BCRP/ABCG2) influences the levels of enterolignans and their metabolites in plasma, milk and mammary gland. *J. Funct. Foods* **35**, 648–654 (2017).

62. Miguel, V. *et al.* Role of ABCG2 in transport of the mammalian lignan enterolactone and its secretion into milk in abcg2 knockout mice. *Drug Metab. Dispos.* **42**, 943–946 (2014).

63. P-Cresol | CH3C6H4OH | CID 2879 - PubChem. https://pubchem.ncbi.nlm.nih.gov/compound/2879#section=Computed-Properties.

64. P-Cresol sulfate | C7H8O4S | CID 4615423 - PubChem. https://pubchem.ncbi.nlm.nih.gov/compound/4615423#section=Computed-Properties.

65. Merino, G. *et al.* Transport of anthelmintic benzimidazole drugs by breast cancer resistance protein (BCRP/ABCG2). *Drug Metab. Dispos.* **33**, 614–618 (2005).

66. Blanco-Paniagua, E., Álvarez- Fernández, L., Garcia-Lino, A. M., Álvarez, A. I. & Merino, G. Secretion into Milk of the Main Metabolites of the Anthelmintic Albendazole Is Mediated by the ABCG2/BCRP Transporter. *Antimicrob. Agents Chemother.* **66**, e0006222 (2022).

67. Álvarez–Fernández, L. *et al.* The ABCG2 protein in vitro transports the xenobiotic thiabendazole and increases the appearance of its residues in milk. *Environ. Toxicol. Pharmacol.* **107**, 104421 (2024).

68. Millán-García, A., Álvarez- Fernández, L., Blanco-paniagua, E., Álvarez, A. I. & Merino, G. The ABCG2 Transporter Affects Plasma Levels , Tissue

Distribution and Milk Secretion of Lumichrome , a Natural Derivative of Riboflavin. *Int. J. Mol. Sci.* **25**, 9884 (2024).

69. van Herwaarden, A. E. *et al.* Multidrug Transporter ABCG2/Breast Cancer Resistance Protein Secretes Riboflavin (Vitamin B2) into Milk. *Mol. Cell. Biol.* **27**, 1247–1253 (2007).

70. Álvarez-Fernández, L. *et al.* ABCG2 transporter plays a key role in the biodistribution of melatonin and its main metabolites. *J. Pineal Res.* **74**, e12849 (2023).

71. Álvarez-Fernández, L., Blanco-Paniagua, E. & Merino, G. ABCG2 Transports the Flukicide Nitroxynil and Affects Its Biodistribution and Secretion into Milk. *Pharmaceutics* **16**, 558 (2024).

72. Perez, M. *et al.* Inhibition of ABCG2/BCRP transporter by soy isoflavones genistein and daidzein: Effect on plasma and milk levels of danofloxacin in sheep. *Vet. J.* **196**, 203–208 (2013).

73. Real, R. *et al.* Involvement of breast cancer resistance protein (BCRP/ABCG2) in the secretion of danofloxacin into milk: Interaction with ivermectin. *J. Vet. Pharmacol. Ther.* **34**, 313–321 (2011).

74. Mizuno, N. *et al.* Impaired renal excretion of 6-hydroxy-5,7-dimethyl-2-methylamino-4-(3- pyridylmethyl) benzothiazole (E3040) sulfate in breast cancer resistance protein (BCRP1/ABCG2) knockout mice. *Drug Metab. Dispos.* **32**, 898–901 (2004).

75. Rybenkov, V. V *et al.* The Whole Is Bigger than the Sum of Its Parts: Drug Transport in the Context of Two Membranes with Active Efflux. *Chem. Rev.* **121**, 5597–5631 (2021).

76. Merino, G., Jonker, J. W., Wagenaar, E., Van Herwaarden, A. E. & Schinkel, A. H. The breast cancer resistance protein (BCRP/ABCG2) affects pharmacokinetics, hepatobiliary excretion, and milk secretion of the antibiotic nitrofurantoin. *Mol. Pharmacol.* **67**, 1758–1764 (2005).

77. Deltombe, O. *et al.* Exploring protein binding of uremic toxins in patients with different stages of chronic kidney disease and during hemodialysis. *Toxins (Basel).* **7**, 3933–3946 (2015).

78. Blanco-Paniagua, E., García-Lino, A. M., García-Mateos, D., Álvarez, A. I. & Merino, G. Role of the Abcg2 transporter in plasma levels and tissue accumulation of the anti-inflammatory tolfenamic acid in mice. *Chem. Biol. Interact.* **345**, 109537 (2021).

79. Garcia-Lino, A. M. *et al.* Abcg2 transporter affects plasma, milk and tissue levels of meloxicam. *Biochem. Pharmacol.* **175**, 113924 (2020).

80. Van Herwaarden, A. E. & Schinkel, A. H. The function of breast cancer resistance protein in epithelial barriers, stem cells and milk secretion of drugs and xenotoxins. *Trends Pharmacol. Sci.* **27**, 10–16 (2006).

81. Pavek, P. *et al.* Human Breast Cancer Resistance Protein : Interactions with Steroid Drugs , Hormones , the Dietary Carcinogen Transport of Cimetidine.

J. Pharmacol. Exp. Ther. **312**, 144–152 (2005).

82. van Herwaarden, A. E. *et al.* Breast cancer resistance protein (Bcrp1/Abcg2) reduces systemic exposure of the dietary carcinogens aflatoxin B1, IQ and Trp-P-1 but also mediates their secretion into breast milk. *Carcinogenesis* **27**, 123–130 (2006).

83. Van De Wetering, K. & Sapthu, S. ABCG2 functions as a general phytoestrogen sulfate transporter in vivo. *FASEB J.* **26**, 4014–4024 (2012).

84. Alfaras, I. *et al.* Involvement of breast cancer resistance protein (BCRP1/ABCG2) in the bioavailability and tissue distribution of trans-resveratrol in knockout mice. *J. Agric. Food Chem.* **58**, 4523–4528 (2010).

85. García-Mateos, D. *et al.* An altered tissue distribution of flaxseed lignans and their metabolites in Abcg2 knockout mice. *Food Funct.* **9**, 636–642 (2018).

86. Takada, T. *et al.* Identification of ABCG2 as an Exporter of Uremic Toxin Indoxyl Sulfate in Mice and as a Crucial Factor Influencing CKD Progression. *Sci. Rep.* **8**, 1–9 (2018).

87. Watanabe, H. *et al.* P-Cresyl sulfate causes renal tubular cell damage by inducing oxidative stress by activation of NADPH oxidase. *Kidney Int.* **83**, 582–592 (2013).

88. Hira, D. & Terada, T. BCRP/ABCG2 and high-alert medications: Biochemical, pharmacokinetic, pharmacogenetic, and clinical implications. *Biochem. Pharmacol.* **147**, 201–210 (2018).

89. Fu, H.-Y. *et al.* The Clostridium Metabolite P-Cresol Sulfate Relieves Inflammation of Primary Biliary Cholangitis by Regulating Kupffer Cells. *Cells* **11**, 3782 (2022).

90. Azevedo, M. L. V. *et al.* p-Cresyl sulfate affects the oxidative burst, phagocytosis process, and antigen presentation of monocyte-derived macrophages. *Toxicol. Lett.* **263**, 1–5 (2016).

91. Shiba, T. *et al.* Effects of intestinal bacteria-derived p-cresyl sulfate on Th1-type immune response in vivo and in vitro. *Toxicol. Appl. Pharmacol.* **274**, 191–199 (2014).

92. Tanaka, Y., Slitt, A. L., Leazer, T. M., Maher, J. M. & Klaassen, C. D. Tissue distribution and hormonal regulation of the breast cancer resistance protein (Bcrp/Abcg2) in rats and mice. *Biochem. Biophys. Res. Commun.* **326**, 181–187 (2004).

93. Pérez, M. *et al.* Milk secretion of nitrofurantoin, as a specific BCRP/ABCG2 substrate, in assaf sheep: Modulation by isoflavones. *J. Vet. Pharmacol. Ther.* **32**, 498–502 (2009).

94. Gunes, Y., Okyar, A., Krajcsi, P., Fekete, Z. & Ustuner, O. Modulation of monepantel secretion into milk by soy isoflavones. *J. Vet. Pharmacol. Ther.* **46**, 185–194 (2023).

95. Otero, J. A. *et al.* Flaxseed-enriched diets change milk concentration of the

antimicrobial danofloxacin in sheep. *BMC Vet. Res.* **14**, 14 (2018).

96. Pruthi, S. *et al.* A phase III, randomized, placebo-controlled, double-blind trial of flaxseed for the treatment of hot flashes: North central cancer treatment group N08C7. *Menopause* **19**, 48–53 (2012).

97. Leti Maggio, E. *et al.* Polyphenols Regulate the Activity of Endocrine-Disrupting Chemicals, Having Both Positive and Negative Effects. *J. Xenobiotics* **14**, 1378–1405 (2024).

98. Mao, Q. & Unadkat, J. D. Role of the Breast Cancer Resistance Protein (BCRP/ABCG2) in Drug Transport—an Update. *AAPS J.* **17**, 65–82 (2015).

99. Sabet, Z. *et al.* Talazoparib Does Not Interact with ABCB1 Transporter or Cytochrome P450s, but Modulates Multidrug Resistance Mediated by ABCC1 and ABCG2: An in Vitro and Ex Vivo Study. *Int. J. Mol. Sci.* **23**, 14338 (2022).

100. Sharma, S., Mettu, V. S. & Prasad, B. Interplay of Breast Cancer Resistance Protein (Bcrp/Abcg2), Sex, and Fed State in Oral Pharmacokinetic Variability of Furosemide in Rats. *Pharmaceutics* **15**, 542 (2023).

101. Yang, H. *et al.* Reversal of ABCG2-mediated drug resistance by tinodasertib (ETC-206). *Front. Pharmacol.* **16**, 1606857 (2025).

102. Polgar, O., Robey, R. W. & Bates, S. E. ABCG2: structure, function and role in drug response. *Expert Opin. Drug Metab. Toxicol.* **4**, 1–15 (2008).

103. Merino, G., Van Herwaarden, A. E., Wagenaar, E., Jonker, J. W. & Schinkel, A. H. Sex-dependent expression and activity of the ATP-binding cassette transporter breast cancer resistance protein (BCRP/ABCG2) in liver. *Mol. Pharmacol.* **67**, 1765–1771 (2005).

104. Blazquez, A. M. G. *et al.* Lactation during cholestasis: Role of ABC proteins in bile acid traffic across the mammary gland. *Sci. Rep.* **7**, 7475 (2017).

105. Patel, K. P., Luo, F. J. G., Plummer, N. S., Hostetter, T. H. & Meyer, T. W. The production of p-Cresol sulfate and indoxyl sulfate in vegetarians versus omnivores. *Clin. J. Am. Soc. Nephrol.* **7**, 982–988 (2012).

106. Barrios, C. *et al.* Gut-microbiota-metabolite axis in early renal function decline. *PLoS One* **10**, 1–9 (2015).

107. Zhou, Y. *et al.* p-Cresol Sulfate Is a Sensitive Urinary Marker of Fecal Microbiota Transplantation and Antibiotics Treatments in Human Patients and Mouse Models. *Int. J. Mol. Sci.* **24**, 14621 (2023).

108. Jonker, J. W. *et al.* Role of breast cancer resistance protein in the bioavailability and fetal penetration of topotecan. *J. Natl. Cancer Inst.* **92**, 1651–1656 (2000).

109. González-Lobato, L. *et al.* Novel in vitro systems for prediction of veterinary drug residues in ovine milk and dairy products. *Food Addit. Contam. - Part A* **31**, 1026–1037 (2014).

110. Real, R. *et al.* Analysis of the effect of the bovine adenosine triphosphate-

binding cassette transporter G2 single nucleotide polymorphism Y581S on transcellular transport of veterinary drugs using new cell culture models. *J. Anim. Sci.* **89**, 4325–4338 (2011).

111. Mahnke, H. *et al.* The ABCG2 efflux transporter in the mammary gland mediates veterinary drug secretion across the blood-milk barrier into milk of dairy cows. *Drug Metab. Dispos.* **44**, 700–708 (2016).

112. Jonker, J. W. *et al.* The breast cancer resistance protein protects against a major chlorophyll-derived dietary phototoxin and protoporphyria. *Proc. Natl. Acad. Sci. U. S. A.* **99**, 15649–15654 (2002).

113. Thakare, R., Chhonker, Y. S., Gautam, N., Alamoudi, J. A. & Alnouti, Y. Quantitative analysis of endogenous compounds. *J. Pharm. Biomed. Anal.* **128**, 426–437 (2016).

114. Taverniers, I., De Loose, M. & Van Bockstaele, E. Trends in quality in the analytical laboratory. II. Analytical method validation and quality assurance. *TrAC - Trends Anal. Chem.* **23**, 535–552 (2004).

ACKNOWLEDGEMENTS

The authors thank A.H. Schinkel (The Netherlands Cancer Institute, Amsterdam, The Netherlands), who kindly provided parental MDCK–II cells and their murine Abcg2 and ABCG2–transduced subclones, as well as Abcg2 knockout mice.

AUTHOR CONTRIBUTIONS

Conceptualization, A.M.-G., E.B.-P. and G.M.; methodology, A.M.-G., L.Á.-F., M.V-C, D.H-Á, Á.L-G, Á.F. and E.B.-P.; investigation and formal analysis, A.M.-G., L.Á.-F, M.V-C, D.H-Á, and Á.L-G; data curation and writing-original draft preparation, A.M.-G.; writing-review and editing, L.Á.-F., E.B.-P. and G.M.; validation, resources and project administration, G.M. and Á.F.; supervision and funding acquisition, G.M. All authors have read and agreed to the published version of the manuscript.

ADDITIONAL INFORMATION

The authors declare no competing interests.

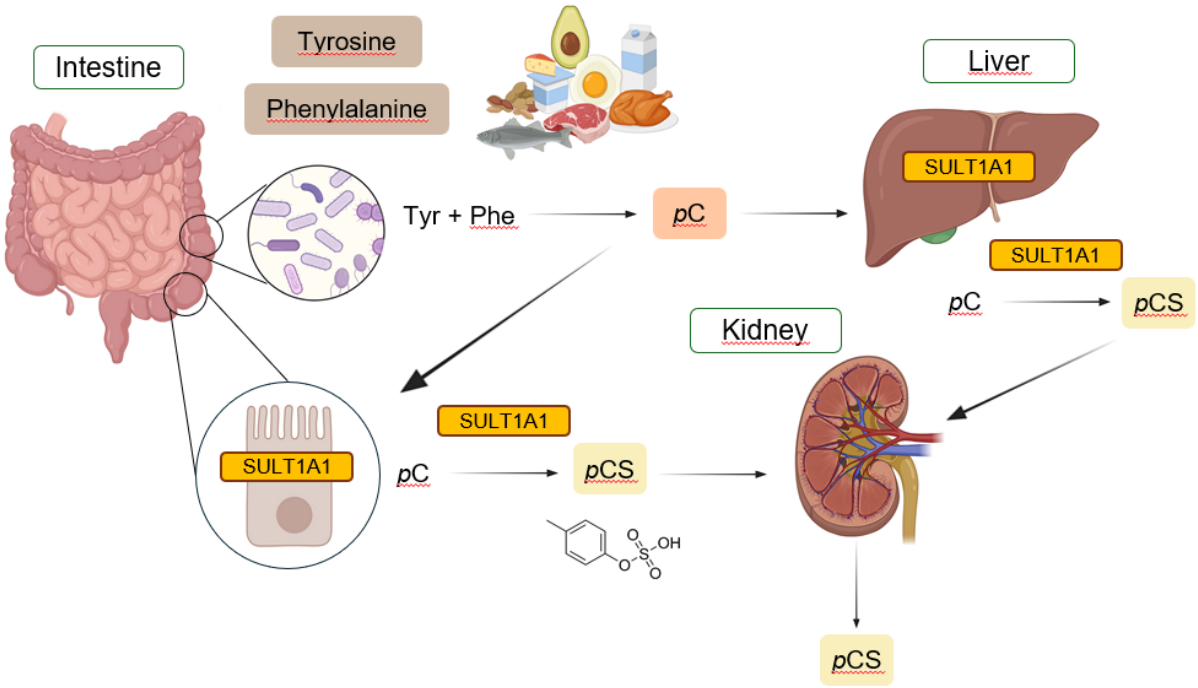

Figure 1. Schematic representation of *p*-cresyl sulfate (*p*CS) metabolism. Tyrosine (Tyr) and phenylalanine (Phe) are dietary aromatic amino acids that are transformed into *p*-cresol (*p*C) in the distal colon through bacterial fermentation. Once formed, *p*C is predominantly converted into *p*CS via sulfation by sulfotransferase 1A1 (SULT1A1), which is abundantly expressed in colonic enterocytes, before being released into the portal circulation. Alternatively, *p*C that escapes intestinal metabolism can be sulfated in the liver, where SULT1A1 is also highly expressed. Finally, *p*CS is eliminated by the kidney and excreted in urine. Created in https://BioRender.com. Based on Blachier and Andriamihaja (2022) [14].

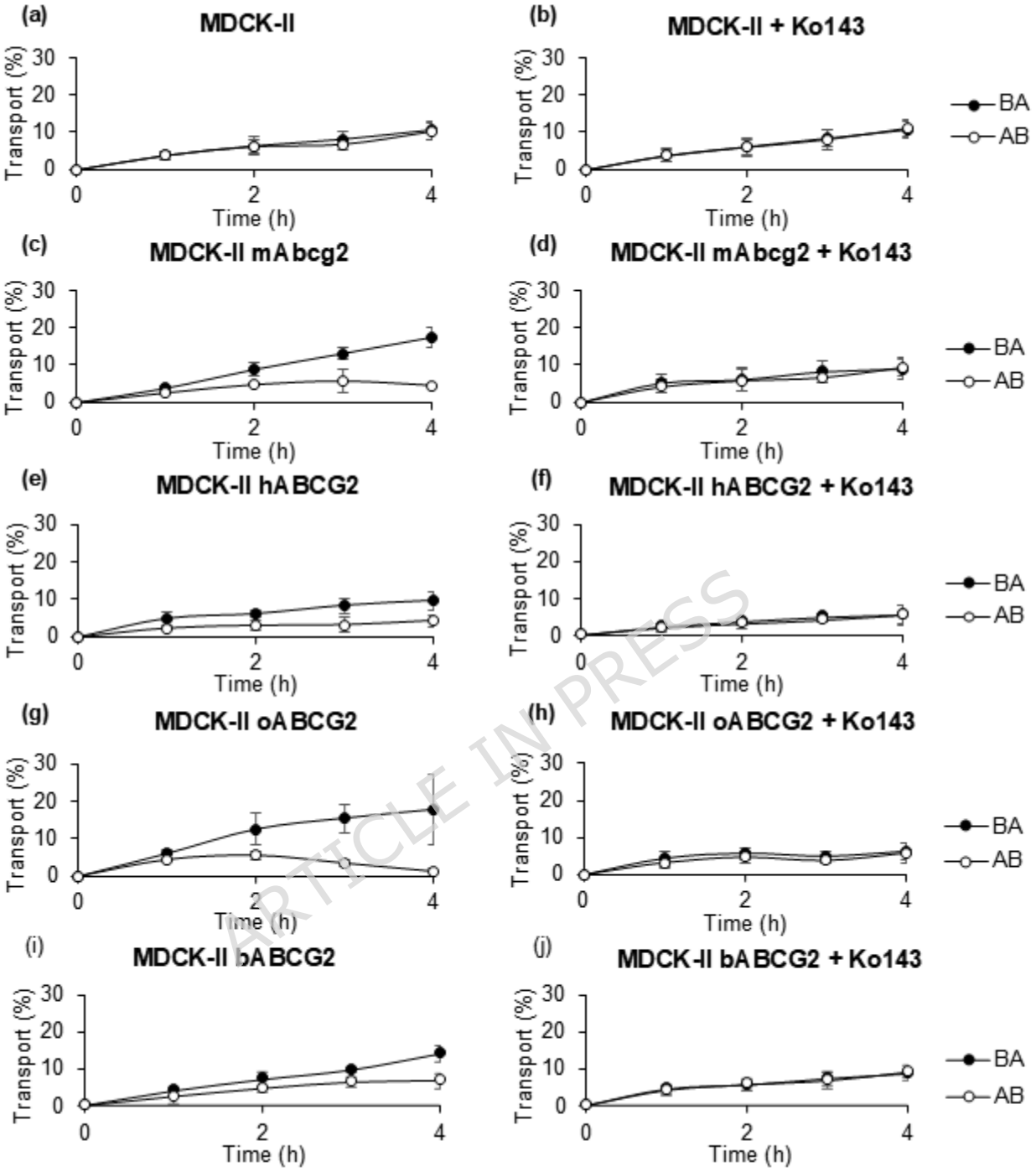

Figure 2. Transepithelial transport assay of *p*-cresyl sulfate (10 μM) in the presence or absence of Ko143 (1 μM), the ABCG2 specific inhibitor, in parental MDCK-II cells (a and b, respectively) and its subclones transduced with murine (mAbcg2) (c and d, respectively), human (hABCG2) (e and f, respectively), ovine (oABCG2) (g and h, respectively) and bovine (bABCG2) (i and j, respectively) variants of the transporter. Initially, medium of both compartments was replaced with fresh culture medium with 10 μM *p*-cresyl sulfate, containing or not the inhibitor. Aliquots were collected at 1, 2, 3 and 4 h on the opposite side where

the potential substrate had been added. All samples were stored at -20°C until being analyzed by ultra-performance liquid chromatography. *p*-Cresyl sulfate detected in the opposite compartment is expressed as the percentage of the total compound added at the beginning of the experiment. (n ≥ 4). Results are shown as mean ± S.D.

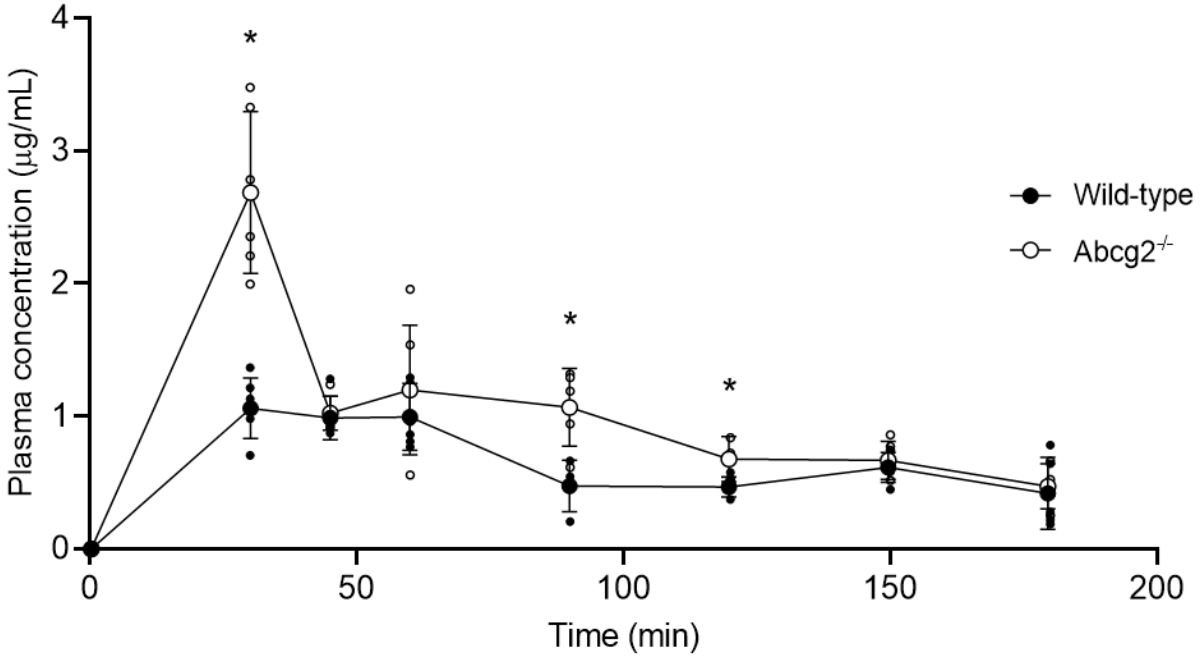

Figure 3. Plasma concentrations of *p*-cresyl sulfate (*p*CS) after oral administration of *p*-cresol (10 mg/kg) in wild-type and Abcg2$^{-/-}$ male mice (n = 4-6). Plasma samples were collected at 30, 45, 60, 90, 120, 150, 180, and 240 min. *p*CS concentrations were quantified by ultra-performance liquid chromatography analysis. Results are presented as individual data and mean ± S.D. *p*CS plasma levels at 240 min were below the limit of quantification. (*) $p \leq 0.05$: significant differences between both groups of mice.

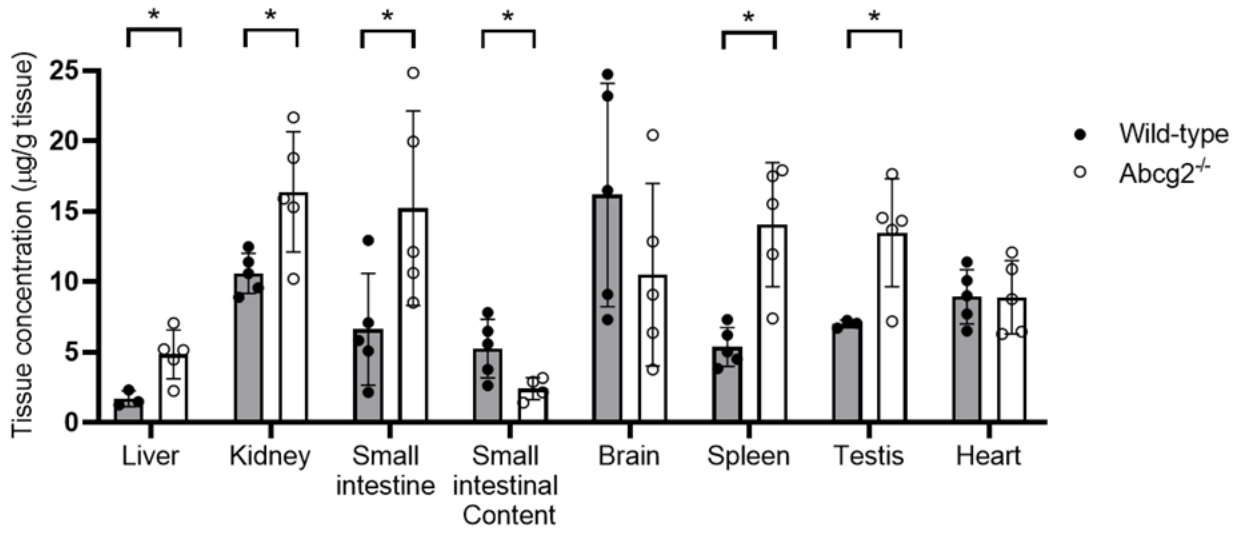

Figure 4. Tissue concentration (µg/g tissue) of *p*-cresyl sulfate in wild-type and Abcg2$^{-/-}$ male mice, measured 2 h after oral administration of the parental molecule, *p*-cresol at a dose of 10 mg/kg body weight (n = 5). Data are shown as individual values and mean ± S.D. (*) $p \leq 0.05$: significant differences between both groups of mice.

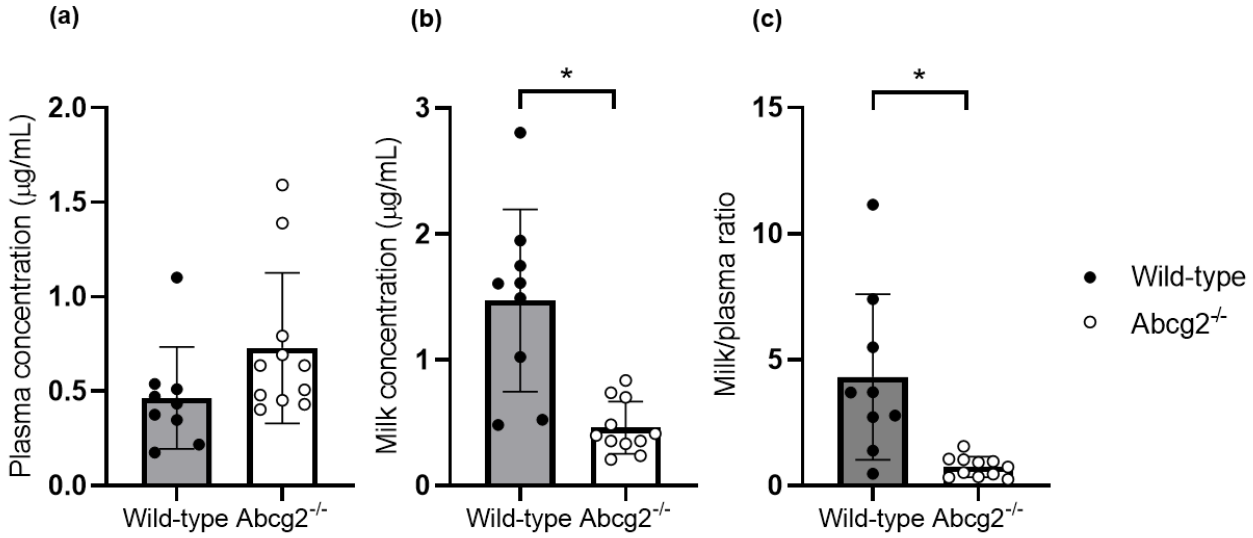

Figure 5. Plasma (a), milk concentration (b), and milk-to-plasma ratio (c) of *p*-cresyl sulfate in wild-type and Abcg2$^{-/-}$ female lactating mice following oral administration of the precursor molecule, *p*-cresol, at a dose of 10 mg/kg (n = 9-11). Plasma and milk samples were collected 2 h after oral administration and concentrations were determined by ultra-performance liquid chromatography. Data are shown as individual values and mean ± S.D. (*) $p \leq 0.05$: significant differences between both groups of mice.

Table 1. Relative efflux transport (BA/AB) ratio, apically directed translocation percentage (%BA transport) divided by basolaterally directed translocation percentage (%AB transport), at 4 h for *p*-cresyl sulfate (10 µM) in parental MDCK-II cells and its subclones transduced with murine (mAbcg2), human ABCG2 (hABCG2), ovine (oABCG2) and bovine (bABCG2) variants, either in the absence (-Ko143) and the presence of the ABCG2 specific inhibitor Ko143 (1 µM) (n ≥ 4).

	-Ko143			**+Ko143**		
	%BA transport	**%AB transport**	**Ratio BA/AB**	**%BA transport**	**%AB transport**	**Ratio BA/AB**
MDCK-II	10.50 ± 2.20	10.18 ± 2.51	1.04 ± 0.10	10.57 ± 2.23	11.03 ± 2.26	0.97 ± 0.10
MDCK-II mAbcg2	17.41 ± 2.50	4.53 ± 0.34	3.83 ± 0.31***	9.03 ± 2.74	9.54 ± 2.61	1.01 ± 0.06$^{\#}$
MDCK-II hABCG2	9.56 ± 2.60	4.22 ± 1.46	2.31 ± 0.28**	5.70 ± 2.70	5.64 ± 2.55	1.00 ± 0.16$^{\#}$
MDCK-II oABCG2	17.84 ± 9.44	1.30 ± 0.82	15.47 ± 4.79**	6.19 ± 2.27	5.99 ± 2.66	1.06 ± 0.13$^{\#}$
MDCK-II bABCG2	14.34 ± 2.24	6.78 ± 2.09	2.21 ± 0.43*	8.68 ± 1.54	9.38 ± 1.67	0.93 ± 0.06$^{\#}$

Results are shown as mean ± S.D. (*) $p \leq 0.05$, (**) $p \leq 0.01$, and (***) $p \leq 0.001$: significant differences in transport ratio compared to parental MDCK-II cells (Student's t-test, normally distributed data). ($^{\#}$) $p \leq 0.05$ significant differences compared to treatment without Ko143 (Student's t-test, normally distributed data).

Figure 1

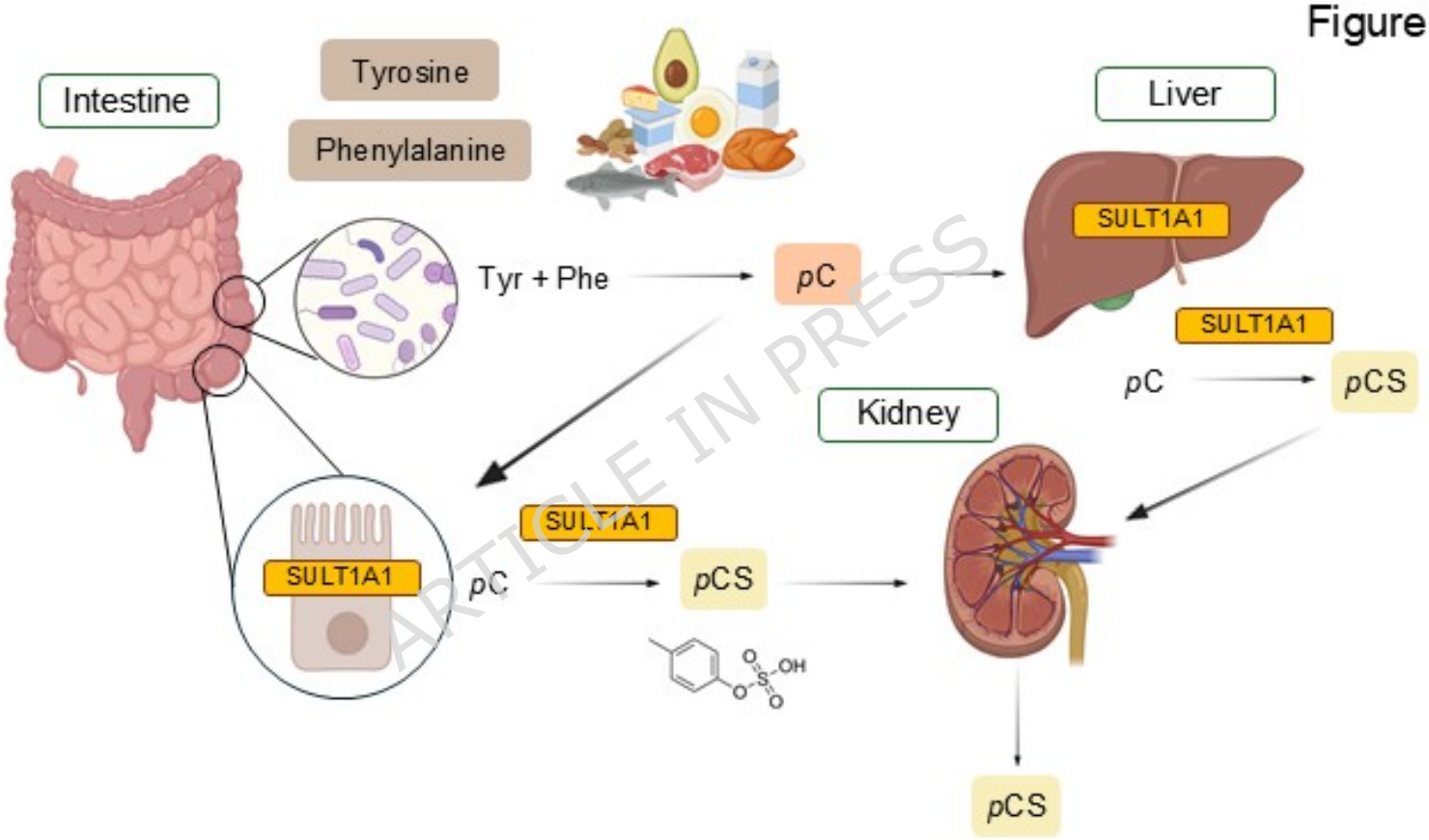

Figure 4

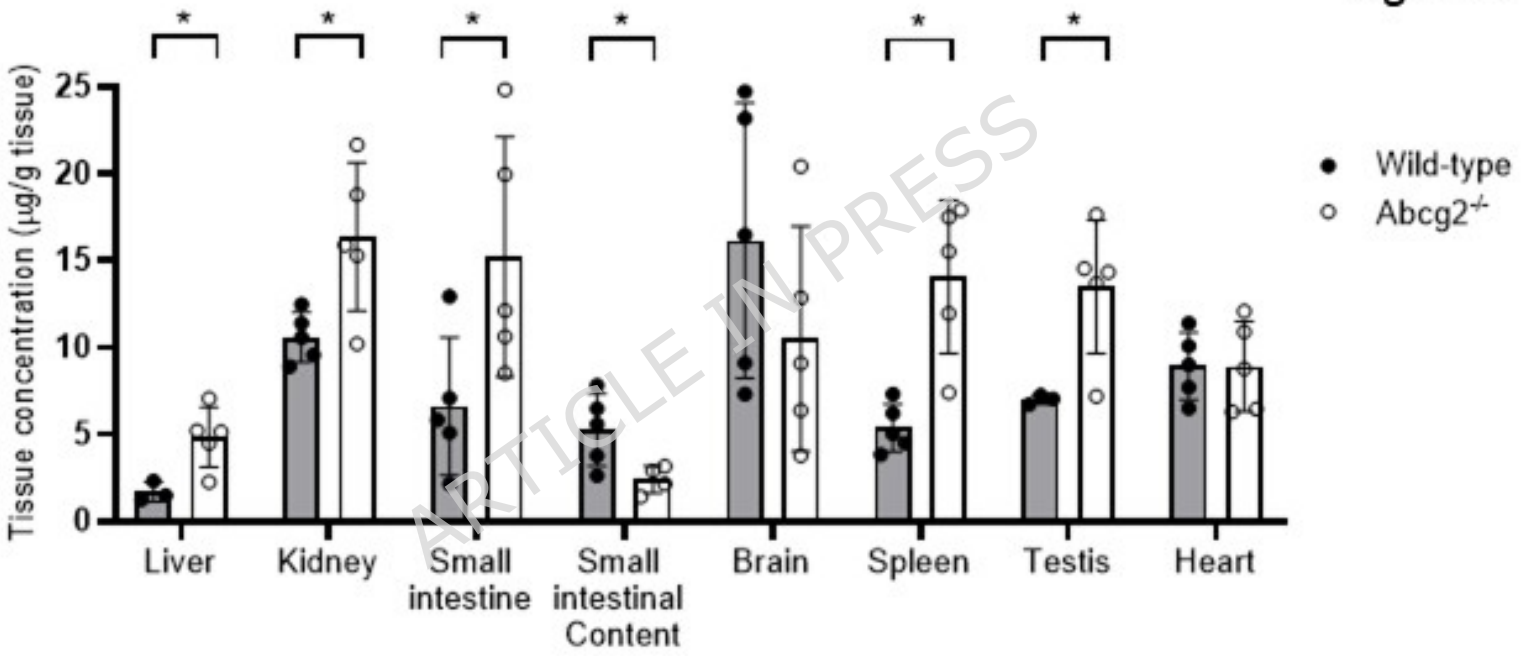

Figure 5

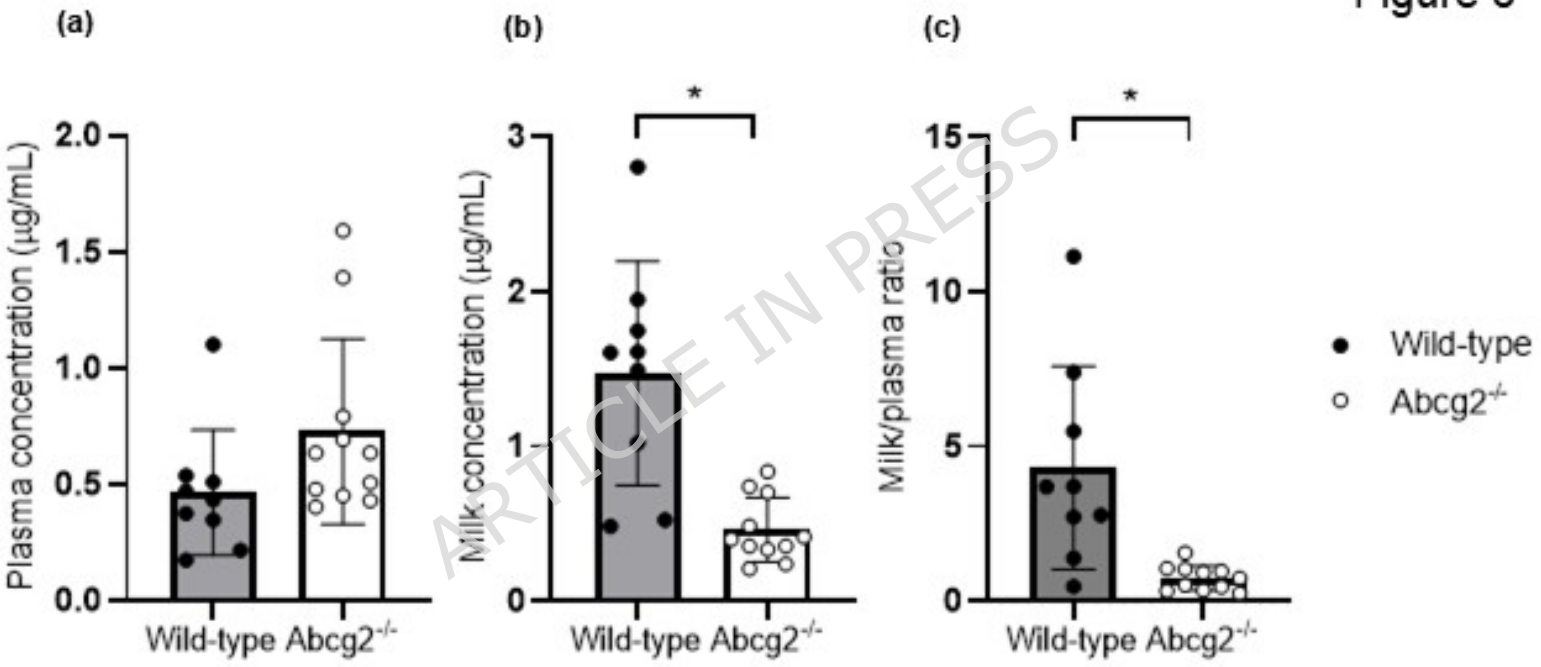

Figure 2

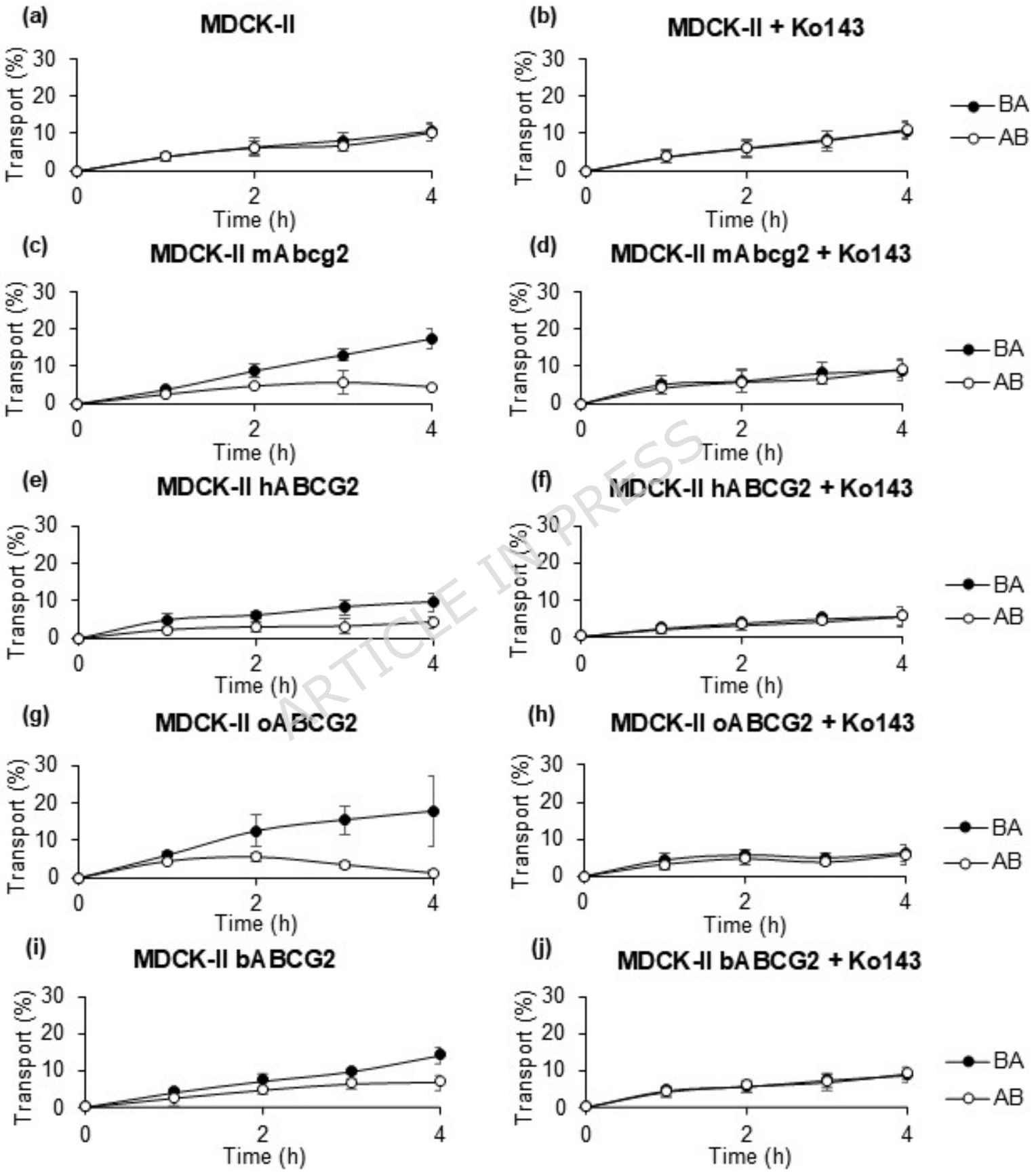

Figure 3

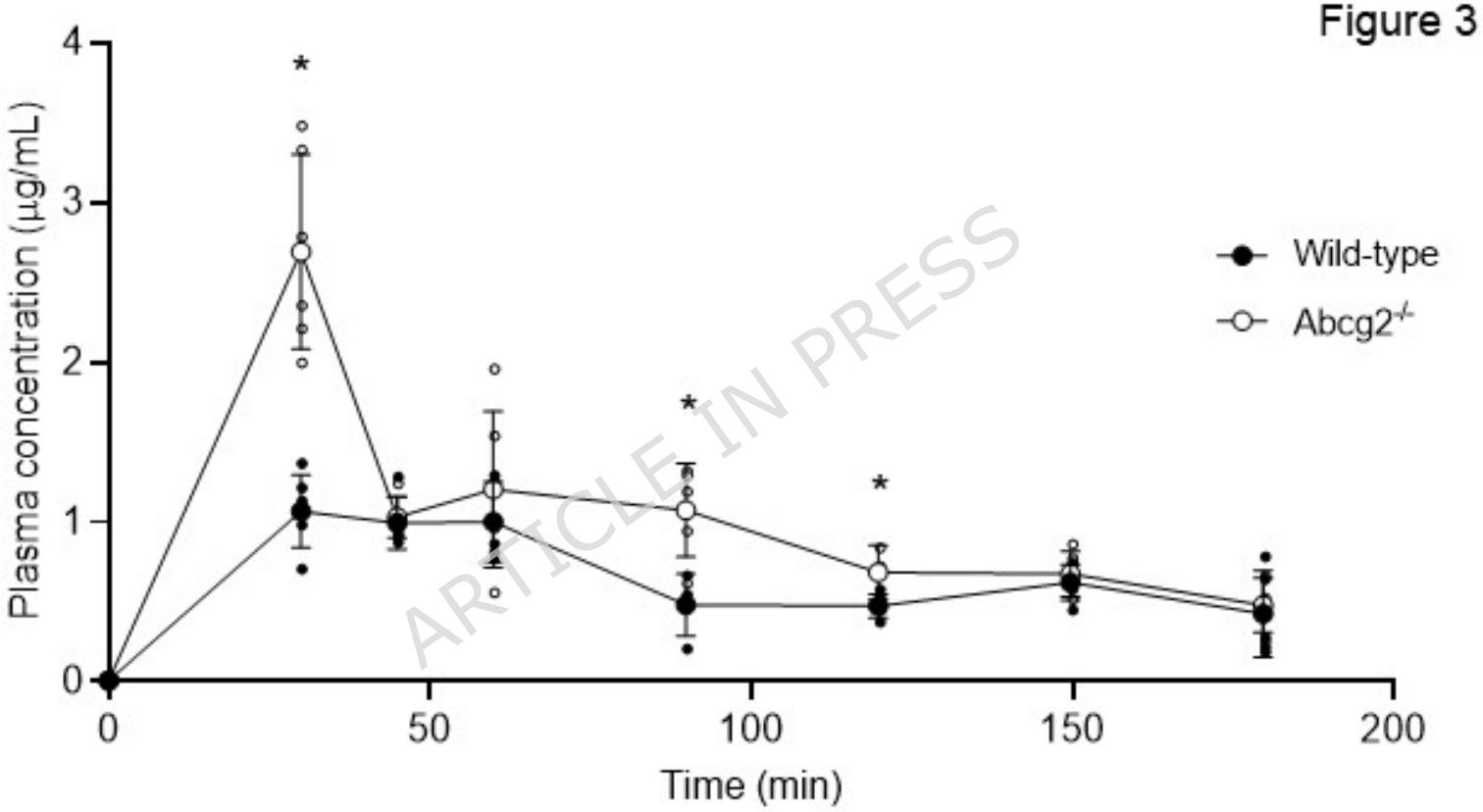

Table 1. Relative efflux transport (BA/AB) ratio, apically directed translocation percentage (%BA transport) divided by basolaterally directed translocation percentage (%AB transport), at 4 h for *p*-cresyl sulfate (10 µM) in parental MDCK-II cells and its subclones transduced with murine (mAbcg2), human ABCG2 (hABCG2), ovine (oABCG2) and bovine (bABCG2) variants, either in the absence (-Ko143) and the presence of the ABCG2 specific inhibitor Ko143 (1 µM) (n ≥ 4).

	-Ko143			**+Ko143**		
	%BA transport	**%AB transport**	**Ratio BA/AB**	**%BA transport**	**%AB transport**	**Ratio BA/AB**
MDCK-II	10.50 ± 2.20	10.18 ± 2.51	1.04 ± 0.10	10.57 ± 2.23	11.03 ± 2.26	0.97 ± 0.10
MDCK-II mAbcg2	17.41 ± 2.50	4.53 ± 0.34	3.83 ± 0.31***	9.03 ± 2.74	9.54 ± 2.61	1.01 ± 0.06#
MDCK-II hABCG2	9.56 ± 2.60	4.22 ± 1.46	2.31 ± 0.28**	5.70 ± 2.70	5.64 ± 2.55	1.00 ± 0.16#
MDCK-II oABCG2	17.84 ± 9.44	1.30 ± 0.82	15.47 ± 4.79**	6.19 ± 2.27	5.99 ± 2.66	1.06 ± 0.13#
MDCK-II bABCG2	14.34 ± 2.24	6.78 ± 2.09	2.21 ± 0.43*	8.68 ± 1.54	9.38 ± 1.67	0.93 ± 0.06#

Results are shown as mean ± S.D. (*) $p \leq 0.05$, (**) $p \leq 0.01$, and (***) $p \leq 0.001$: significant differences in transport ratio compared to parental MDCK-II cells (Student's t-test, normally distributed data). (#) $p \leq 0.05$ significant differences compared to treatment without Ko143 (Student's t-test, normally distributed data).